

## Cytoreductive Surgery and Intraoperative Administration of Paclitaxel-loaded Expansile Nanoparticles Delay Tumor Recurrence in Ovarian Carcinoma

Denis Gilmore, MD<sup>1</sup>, Morgan Schulz, MD<sup>1</sup>, Rong Liu, MD, PhD<sup>1</sup>, Kimberly Ann V. Zubris, PhD<sup>4</sup>, Robert F. Padera, MD<sup>2</sup>, Paul J. Catalano, ScD<sup>3</sup>, Mark W. Grinstaff, PhD<sup>4</sup>, and Yolonda L. Colson, MD, PhD<sup>1</sup>

<sup>1</sup>Division of Thoracic Surgery, Department of Surgery, Brigham and Women's Hospital, Boston, MA; <sup>2</sup>Department of Pathology, Brigham and Women's Hospital, Boston, MA; <sup>3</sup>Department of Biostatistics and Computational Biology, Dana-Farber Cancer Institute, Boston, MA; <sup>4</sup>Departments of Biomedical Engineering and Chemistry, Boston University, Boston, MA

### ABSTRACT

**Background.** Locoregional recurrence significantly impacts survival and quality of life in patients with ovarian carcinoma. We hypothesize that local administration of paclitaxel-loaded expansile nanoparticles (pax-eNP) at the time of cytoreductive surgery decreases local tumor recurrence.

**Methods.** In vitro cytotoxicity of pax-eNP was assessed against both the OVCAR-3 human ovarian cancer cell line and tumor cells isolated from a malignant pleural effusion from a patient with multidrug-resistant ovarian cancer. A murine xenogenic model involving surgical cytoreduction of established OVCAR-3 intra-abdominal tumor was used to evaluate in vivo efficacy of intraoperative intraperitoneal (IP) injection of 10 mg/kg of paclitaxel either as pax-eNP or paclitaxel in Cremophor EL/ethanol solution (pax-C/E) versus empty eNP controls. Cytoreductive surgery and intraoperative treatment were performed 4 weeks after established tumor. All animals were sacrificed when empty eNP controls displayed extensive evidence of disease progression.

**Results.** Labeled-eNP entered tumor cells in vitro within 4 h and specifically accumulated at sites of tumor in vivo. Pax-eNP exhibited dose-dependent cytotoxicity in both OVCAR-3 and patient tumor cells isolated from a malignant pleural effusion and effectively prevented tumor recurrence following debulking ( $p = 0.003$  vs. empty eNP). Furthermore, pax-eNP-treated animals did not develop severe recurrent carcinomatosis compared with 43 % of the pax-C/E-treated cohort, suggesting that single-dose intracavitary pax-eNP is more effective than an equivalent dose of pax-C/E.

**Conclusions.** Expansile nanoparticles readily enter human ovarian tumor cells and localize to sites of tumor in vivo with pax-eNP cytotoxicity resulting in superior inhibition of locoregional tumor recurrence following cytoreductive surgery.

Given the absence of early symptoms or reliable screening, 75 % of women diagnosed with epithelial ovarian cancer present with advanced disease characterized by peritoneal implants or distant metastases.<sup>1</sup> Inability to effectively treat this disease has resulted in more deaths from ovarian cancer than any other female reproductive cancer.<sup>2-4</sup> Clinical course is dominated by locoregional extension, with death ultimately occurring from progressive intraperitoneal disease. The current standard of care consists of cytoreductive surgery and combination platinum/paclitaxel systemic chemotherapy, with intraperitoneal (IP) chemotherapy delivery via an implanted catheter.<sup>5-10</sup> Despite this aggressive approach, overall 5-year survival remains less than 50 % secondary to the high incidence of local recurrence attributed to occult residual tumor.<sup>3</sup>

**Electronic supplementary material** The online version of this article (doi:10.1245/s10434-012-2696-5) contains supplementary material, which is available to authorized users.

© Society of Surgical Oncology 2012

First Received: 8 February 2012

D. Gilmore, MD  
e-mail: dgilmor1@bidmc.harvard.edu

Published online: 06 November 2012

Although multiple IP boluses of chemotherapeutic agents, most notably paclitaxel, can significantly decrease local tumor recurrence and increase survival, more than half of patients are unable to complete therapy due to peritoneal adhesions, bowel obstructions, infections, and catheter-related complications.<sup>8</sup> These findings suggest that concentrating paclitaxel delivery directly within tumor cells in a local, controlled-release fashion without bolus kinetics or catheter delivery could significantly decrease systemic toxicity and markedly improve patient outcome and quality. Therefore, various formulations of nanoparticles have been proposed as a novel means to treat ovarian cancer. However, many successful *in vitro* formulations have been ineffective against tumor growth when tested *in vivo*, and others were associated with significant intraperitoneal adhesions. Studies utilizing malignant cell lines of various origins including ovarian (OVCAR3, SW626, and SKOV-3), pancreatic (BxPC-3), lung (TC-1), and mesothelioma cells (MSTO-211H) have all demonstrated superior *in vitro* efficacy of nanoparticle therapy compared with standard treatment. However, only the mesothelioma study, which uses the nanoparticle formulation investigated in the current study, demonstrated superior *in vivo* efficacy over comparative drug therapy.<sup>11–15</sup> We hypothesized that development of a drug-loaded nanoparticle designed for intracellular drug delivery and localization to sites of residual tumor after cytoreduction *in vivo* would result in the benefit of intraperitoneal delivery of paclitaxel without the complications which currently limit therapy.

To deliver drugs in a controlled-release fashion directly to tumor sites, pH-triggered nanoparticles were evaluated for *in vitro* efficacy against an established ovarian carcinoma cell line (OVCAR-3) and against tumor cells isolated from a malignant pleural effusion from a patient with multidrug resistant ovarian cancer, whereas *in vivo* efficacy was evaluated in a novel ovarian xenograft mouse model of cytoreductive surgery. This article demonstrates that the application of pH-triggered expansile nanoparticles for locoregional drug delivery results in localization of chemotherapeutic agents to sites of tumor *in vivo* with superior inhibition of tumor growth and recurrence following surgical cytoreduction in ovarian carcinomatosis.

## MATERIALS AND METHODS

### *Nanoparticle Production*

Empty and paclitaxel-loaded expansile nanoparticles (eNP and pax-eNP) were prepared by using a previously published mini-emulsion polymerization technique with paclitaxel (5 % wt/wt; MP Biomedicals, Solon, OH) dissolved in a methacrylate monomer solution. The emulsified

mixture was polymerized and dialyzed against 5 mM, pH 8.5 phosphate buffer to remove excess surfactant and salts.<sup>16</sup>

### *Cell Lines*

Human ovarian cancer cell line OVCAR-3 (ATCC, Manassas, VA), OVCAR-3 cell line transduced with luciferase (OVCAR-3/luc, a generous gift from J. Rheinwald at Harvard Medical School, Boston, MA), and tumor cells isolated from a malignant pleural effusion in a patient with multi-drug-resistant ovarian cancer were cultured in complete media using Roswell Park Memorial Institute (RPMI) media, containing 10 % (v/v) fetal bovine serum, streptomycin (100 µg/ml), and penicillin (100 units/ml).

### *In Vitro Cytotoxicity*

Human ovarian tumor cells were plated  $3 \times 10^3$  cells/well in complete media. After 24 h, media containing 5 % pax-eNP, empty eNP, or equivalent doses of paclitaxel dissolved in cremophor EL/ethanol based on encapsulation efficiencies replaced previous media. Cytotoxicity at 7 days was assessed via a standard 3-(4,5-dimethylthiazol-2-yl)2,5-diphenyl tetrazolium bromide (MTT) viability assay using spectrophotometric quantification at 570 nm (Invitrogen; Carlsbad, CA). Triplicate assays were performed and percent viability calculated as absorbance relative to treatment-free controls. Data are presented as mean  $\pm$  standard error.

### *Cellular Uptake*

OVCAR-3 tumor cells were plated  $10^5$  cells/well in complete media. After 24 h, media was replaced with 50 µg/ml rhodamine labeled eNP (rho-eNP) in complete media. Cells were treated for 4, 12, and 24 h and fixed in 3.7 % paraformaldehyde in phosphate buffer saline (PBS) buffer. Following fixation, samples were washed and resuspended in PBS and 0.1 % sodium azide. Cellular uptake of rho-eNP was detected using flow cytometric analysis using the PE-Texas Red channel (LSRFortessa, BD Biosciences, Bedford, MA).

### *Confocal Microscopy*

OVCAR-3 tumor cells were cultured in complete media on a sterile polylysine coated glass coverslip. After 24 h, cells were treated with rho-eNP or media alone for 4, 8, or 24 h. Coverslips were incubated with 1 mL of wheat germ agglutinin Oregon GreenR 488 conjugate (5 µg/ml) and Hoeschst (1:5000) in Hank's Balanced Salt Solution

(HBSS; Invitrogen, Oregon) for 10 min to stain the cell membrane and nuclei, respectively. Cells were imaged on the Zeiss LSM510 scanning confocal laser microscope at Beth Israel Deaconess Medical Center Confocal Imaging Core.

### *Murine Model*

This model is the first to investigate nanoparticle efficacy following cytoreductive surgery in ovarian carcinomatosis, being an adaptation from previously reported carcinomatosis models and our previously described murine cytoreductive surgical model of peritoneal mesothelioma.<sup>17–19</sup> Studies were approved by the Dana-Farber Cancer Institute IACUC. Briefly, nude, female mice (Nu/J; Jackson Laboratories) were maintained in a specific pathogen-free animal facility. Mice (22–26 g) underwent intraperitoneal injection of  $10^6$  OVCAR-3 or OVCAR-3/luc cells. Four weeks after established disease, operative debulking consisting of midline laparotomy, oophorectomy, omentectomy, and resection of macroscopic tumor nodules was performed. Animals were treated with empty eNP or with 10 mg/kg IP of paclitaxel delivered as bolus pax-C/E or pax-eNP at fascial closure. Disease progression was monitored weekly with clinical assessment of drug toxicity, weight loss, ascites, and evidence of intra-abdominal tumor. All animals were sacrificed when non-drug controls displayed evidence of disease progression. Given that empty eNP animals received no drug treatment, we used the extent of tumor present in these untreated animals to define the limits of “severe carcinomatosis,” although this cutoff was not used for statistical analysis. For bioluminescent imaging studies, mice received an IP injection of 2.25 mg firefly luciferin before sacrifice and were imaged with a Xenogen IVIS-50 bioluminescence camera (Caliper Life Sciences, Hopkinton, MA) using a 10 s exposure time.

### *In Vivo Localization of eNP to Tumor Sites*

To assess whether eNP localized to recurrent tumor in vivo in a timely fashion, we needed significant tumor bulk at 7 days. We wanted a slightly larger tumor bulk to study, and therefore, female (Nu/J) mice received a slightly larger tumor inoculation of  $10^7$  OVCAR-3/luc cells IP. Seven days later when tumor growth was established, 500  $\mu$ l of rho-eNP were given IP. Bioluminescent imaging was performed 24 h later before sacrifice at which time bioluminescent areas were used to identify areas of gross tumor. Animals were then imaged under UV light to identify sites of rho-eNP and to establish specific localization to sites of established tumor.

### *Statistical Analysis*

In vitro studies were compared by using analysis of variance (ANOVA). All in vivo studies were analyzed by using exact nonparametric methods: the Kruskal–Wallis test (comparing >2 groups), the Wilcoxon rank-sum test (comparing 2 groups), or variance ratio test. All testing was two-sided.

## **RESULTS**

### *Pax-eNP Kill OVCAR-3 Human Ovarian Tumor Cells in Vitro*

Dose-dependent antitumor activity of 5 % pax-eNP was assessed against OVCAR-3 in a 7 day in vitro cytotoxicity assay. Pax-eNP and standard paclitaxel control (pax-C/E) exhibited equivalent dose-dependent activity against OVCAR-3 (Fig. 1). Drug concentrations of 10 ng/ml or greater were effective for both pax-eNP or pax-C/E. Pax-eNP cytotoxicity was due to the presence of paclitaxel rather than toxicity of the polymer, as tumor cell exposure to empty eNP did not significantly decrease cell viability.

### *Pax-eNP Exhibit Anti-Tumor Efficacy Against a Malignant Human Pleural Effusion*

Pax-eNP demonstrated superior cytotoxicity compared with pax-C/E when tested ( $n = 3$ ) against fresh human ovarian cancer cells obtained from a malignant pleural effusion of a patient with multidrug-resistant papillary serous ovarian carcinoma (Fig. 1). Clinical resistance was documented against paclitaxel, carboplatin, gemcitabine, bevacizumab, vinorelbine, and an experimental angiogenic kinase inhibitor. Pax-eNP exhibited superior tumor cytotoxicity compared to conventional pax-C/E control ( $p < 0.001$ ) at concentrations of 10 ng/ml and above, similar to the effective dose range identified against OVCAR. Again, empty eNP did not demonstrate tumor cell toxicity, confirming tumor cell death in a human pleural effusion is also due to drug release from pax-eNP rather than the polymer itself.

### *OVCAR Tumor Cell Uptake of eNP*

Given the improved efficacy of pax-eNP against tumor cells previously deemed paclitaxel-resistant, we hypothesized that pax-eNP enter and remain within the tumor cell allowing prolonged exposure to paclitaxel. To answer this question, cellular uptake studies of rhodamine-labeled eNP (rho-eNP) within OVCAR-3 tumor cells were performed using flow cytometry to determine eNP uptake and persistence within

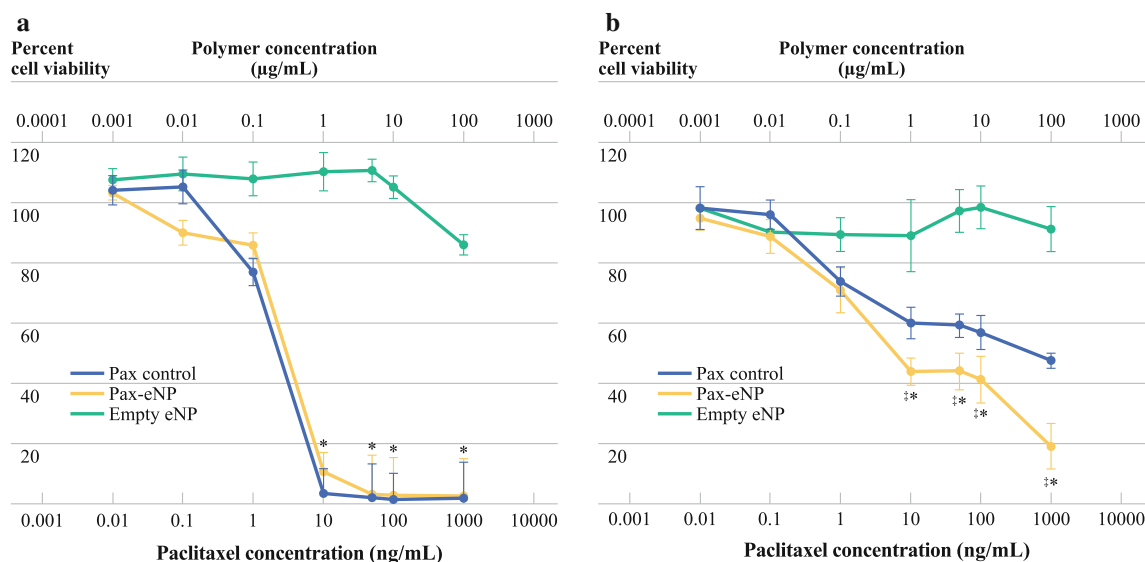


**FIG. 1** Paclitaxel-loaded expansile nanoparticles are effective against OVCAR-3 (a) tumor cells in vitro and superior in vitro against fresh human ovarian cancer cells (b) derived from a malignant pleural effusion in multidrug-resistant papillary serous ovarian carcinoma. Dose titration curve demonstrating dose dependent antitumor activity of pax-eNP and pax control in vitro against

the cell. Time-dependent uptake of rho-eNP was assessed at 4, 12, and 24 h. Increased fluorescence due to rho-eNP uptake is visualized within OVCAR-3 cells starting at 4 h, further increases by 12 h, and begins to decrease slightly by 24 h, suggesting a small amount of rho-eNP exocytosis may be occurring by this time (Fig. 2a). These results demonstrate continued uptake of rho-eNP for at least 12 h with continued intracellular presence at 24 h, a significantly longer exposure time than that previously reported for paclitaxel alone.<sup>20</sup>

Confocal imaging was performed to confirm that rho-eNP were distributed inside OVCAR tumor cells. Consistent with the flow cytometric studies, the images reveal cellular uptake of rho-eNP at 4 h and continued presence at 24 h (Fig. 2c, d).

#### *Pax-eNPs Given After Cytoreductive Surgery Prevent Tumor Recurrence in Vivo*

Having demonstrated pax-eNP efficacy in vitro, we assessed whether pax-eNP delayed local recurrence of ovarian cancer in vivo after primary tumor resection. Surgical debulking of xenogeneic tumor implants was achieved with <3-mm residual tumor in >95 % of animals with a <10 % operative mortality. We compared the postsurgical efficacy of 10 mg/kg intraperitoneal (IP) paclitaxel doses formulated as pax-eNP ( $n = 11$ ) versus clinically used paclitaxel in Cremophor/Ethanol (pax-C/E,  $n = 7$ ). An equivalent polymer dose of empty eNP ( $n = 6$ ) was used as a

OVCAR-3 cells and fresh human ovarian cancer cells derived from a malignant pleural effusion after 7-day exposure analyzed using the MTT cytotoxicity assay. Representative example of  $n = 3$ . \* $p < 0.001$  for pax-eNP and pax-C/E versus empty eNP and † $p < 0.001$  for pax-eNP versus pax-C/E

negative control. Trends in animal weight following treatment are depicted in Fig. 3a. There was a decrease in animal weight in the empty eNP group as expected given the extensive tumor growth in these animals, whereas pax-eNP animals did not lose weight. Significant ascites was not noted in any treatment group. At 4 weeks after surgical debulking and treatment, significant carcinomatosis was seen in animals treated with empty eNP (2.67 g, SD  $\pm$  2.28 g; Table 1), prompting sacrifice of the entire cohort for comparative analysis (Fig. 3). The degree of tumor take, and thus tumor bulk at the time of sacrifice, often was variable among animals, secondary to rate of tumor adherence and growth. All untreated (i.e., empty eNP) animals exhibited 0.57 g of tumor or greater thus establishing our cutoff for severe carcinomatosis. The use of bioluminescence tumor helped to identify areas of tumor and minimize the inclusion of surrounding inflammatory tissue during the resection of tumor specimen. Bioluminescent imaging studies demonstrate direct correlation to tumor burden confirming true tumor (Fig. 4). To demonstrate that the bioluminescent areas were tumor, representative H + E images of tumor nodules are included in the manuscript (Fig. 5c). Nearly all animals treated with empty eNP and many pax-C/E-treated animals exhibited evidence of severe recurrent carcinomatosis. Comparison of the mass of recurrent tumor present in each group at the time of sacrifice revealed a significant decrease with pax-eNP or pax-C/E treatments compared with empty eNP following cytoreductive surgery (Fig. 3;  $p = 0.003$  and  $p = 0.015$ , respectively). As in clinical patients, pax-C/E

**FIG. 2** OVCAR Cell uptake of rho-eNP. **a** Flow cytometric analysis demonstrates rho-eNP uptake within 4 h and continued intracellular presence at 24 h. **b, c,** and **d** Confocal images of rho-eNP particles (red) within OVCAR-3 tumor cells stained for cell membranes (green) and nucleus (blue). **b** Represents negative control and treatment with rho-eNP after 4 h (**c**) and 24 h (**d**) of exposure

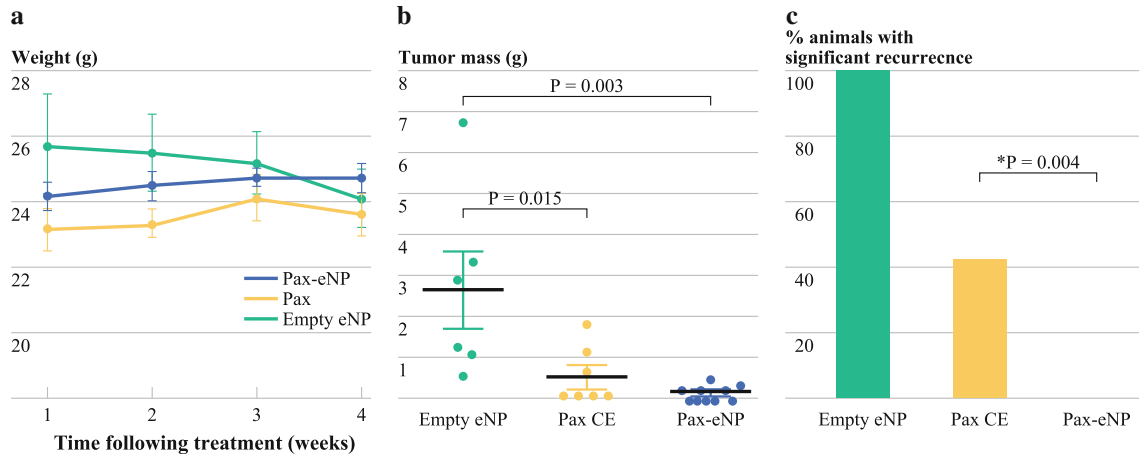
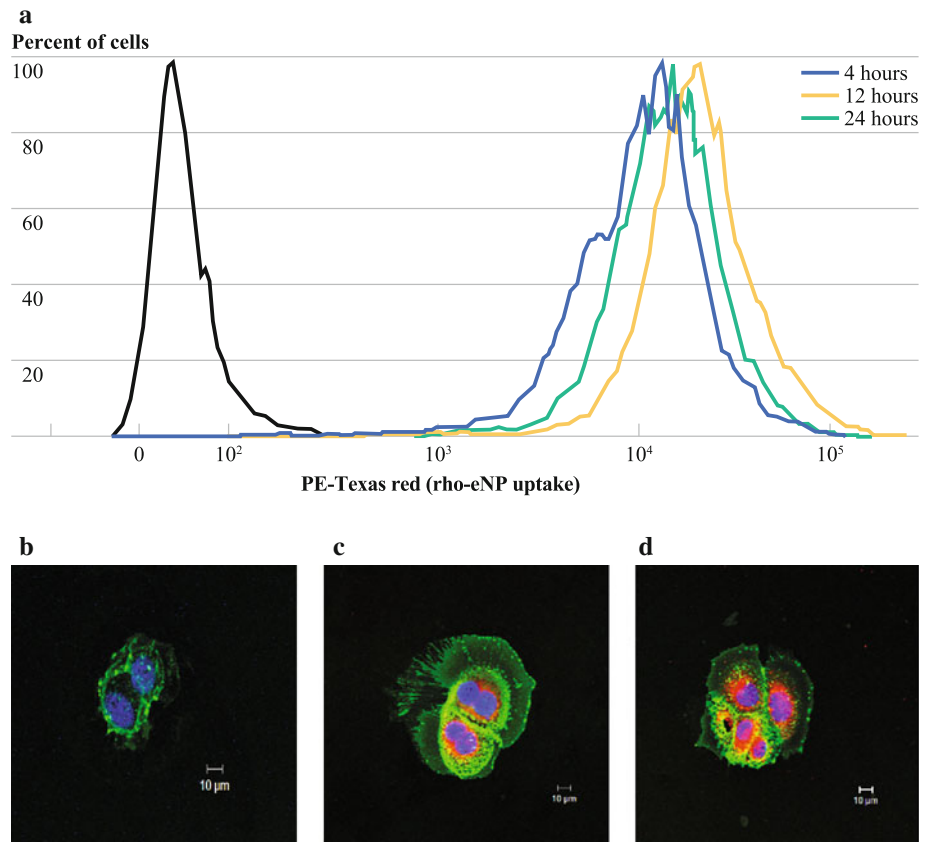


**FIG. 3** **a** Animal weight decreased weekly following treatment with empty-eNP and pax compared with weight gain in the pax-eNP treatment group. To quantify the difference seen on gross examination, total tumor mass and percent of animals with significant tumor

recurrence characterized as  $>0.5$  g of tumor mass were compared. **b** Significant reduction in tumor mass following surgical debulking and treatment with pax-eNP and pax-C/E. **c** Decrease in the percentage of pax-eNP treated animals with significant recurrence

treated animals exhibited variable response to treatment with an average tumor mass of  $0.53 \text{ g} \pm 0.73$ , highlighting this variability. In comparison, the average tumor mass for pax-eNP treated animals was much smaller and more consistent at  $0.15 \text{ g} \pm 0.19$ . Given that division of pax-C/E animals fall into low recurrence versus severe recurrence groups, we used a post hoc analysis to compare the difference between the

variances of pax-C/E and pax-eNP treatment groups. Bimodal distribution in the pax-C/E population demonstrated 43 % of animals with disease equivalent to untreated controls (i.e.,  $>0.57$  g), whereas no animals in the pax-eNP group (0/11) had tumor burden greater than this level ( $p = 0.0003$ , variance ratio 15.7). These findings confirm the difference evident in vivo on gross imaging, whereby 10 mg/kg



**TABLE 1** Recurrent tumor mass

	Empty eNP	Pax-CE	Pax-eNP
	1.27	0.63	0.24
	2.92	1.18	0
	0.57	1.83	0.24
	3.38	0	0.55
	6.75	0.03	0
	1.1	0.01	0.02
		0	0.2
			0
			0.07
			0.38
			0.01
SD	2.28	0.73	0.19

pax-eNP demonstrated a marked decrease in severe recurrent disease compared with equivalent bolus dosing of pax-C/E. Of note, IP treatment with pax-eNP was well tolerated without development of adhesions in any animals.

#### *In vivo Localization of eNP to Sites of Carcinomatosis*

Given the superior prevention of severe recurrent disease in vivo and the prior demonstration of tumor cell uptake in vitro, we investigated whether pax-eNP localized

to areas of tumor in vivo using UV imaging of rho-eNP administered after 7 days of tumor establishment. Rho-eNP were injected IP and animals were sacrificed 24 h later with UV imaging of the open abdomen to identify areas of rho-eNP accumulation. Preferential accumulation of rho-eNP occurred exclusively at known sites of tumor (Fig. 5). These findings suggest that in vivo efficacy of pax-eNP was enhanced by an affinity of eNP for sites of tumor, thereby locally concentrating paclitaxel drug delivery within the tumor, rather than nondiscriminate delivery throughout the peritoneal cavity as occurs with pax-C/E, which is rapidly cleared.

## DISCUSSION

Ovarian cancer often is diagnosed at an advanced stage with the standard of care being cytoreductive surgery plus intravenous and/or intraperitoneal chemotherapy.<sup>21–25</sup> Success is limited by frequent tumor recurrence, poor survival, and high incidence of catheter-related complications. Novel approaches to decrease morbidity and increase efficacy of drug delivery are critically important to advances in care. To our knowledge, morbidity and drug efficacy of nanoparticle-mediated drug delivery has not been assessed preclinically in a relevant cytoreductive surgical model of ovarian cancer. Furthermore, most studies investigating nanoparticle drug delivery have

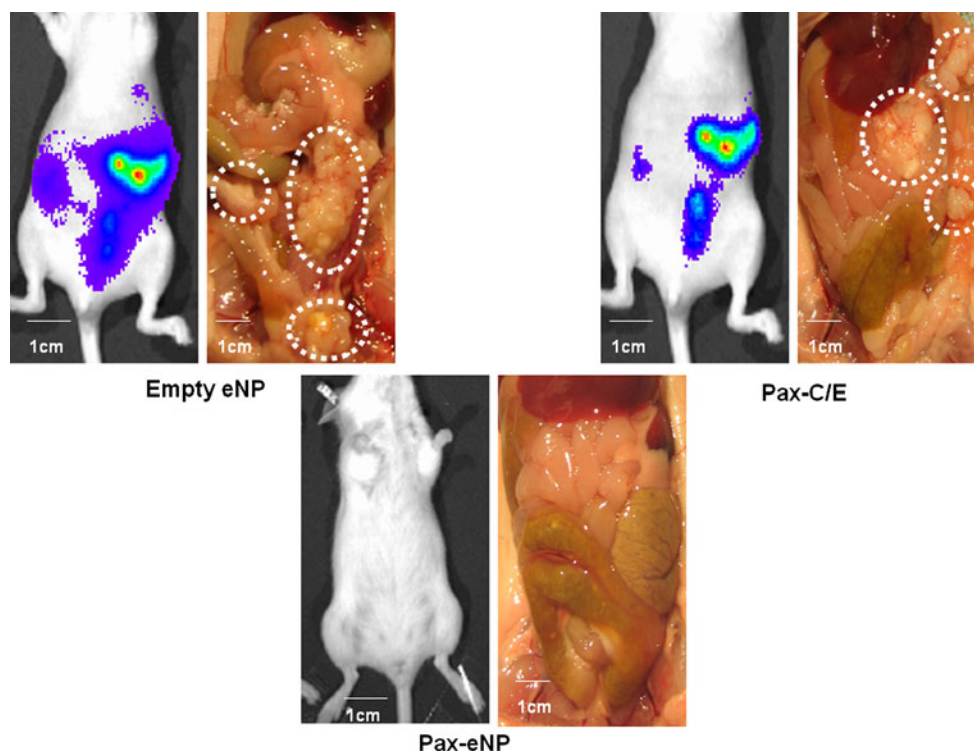


**FIG. 4** Corresponding bioluminescent imaging and gross images of abdomen following surgical debulking and treatment. Pax-eNP effectively prohibited local tumor recurrence. *White circles* highlight tumor burden present in empty eNP and pax-C/E treated animals. *Scale bar* is 1 cm

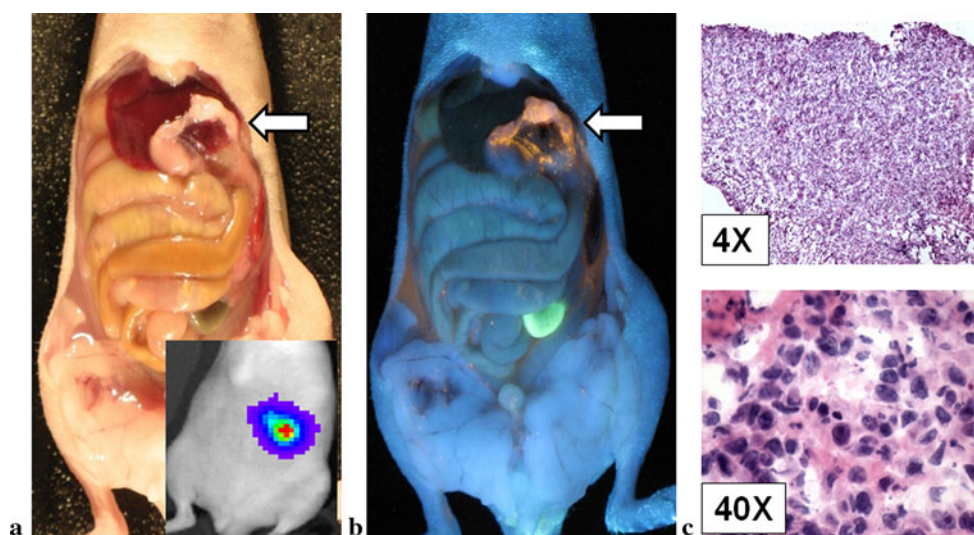


**FIG. 5** **a** Gross imaging of the abdomen demonstrating established tumor. *Inset* depicts corresponding bioluminescent imaging. **b** UV imaging of the abdomen demonstrating fluorescent rho-eNP localization at sites of established tumor (yellow). (White arrows

correspond to same area of tumor in each image). Images are representative of three separate experiments. **c** Histological confirmation of ovarian tumor at low power  $\times 4$  (*top*) and high-power  $\times 40$  (*bottom*)

explored intravenous approaches to systemic delivery and have noted significant entrapment of nanoparticles within the liver and spleen without exclusive localization to tumor.<sup>26</sup> In contrast, we performed cytoreductive surgery and demonstrated immediate IP treatment with pax-eNP results in low incidence of tumor recurrence, low morbidity, and essentially exclusive localization of drug at sites of tumor. There was no visible evidence of uptake within the reticuloendothelial system, including liver and spleen.

Earlier animal studies using various drug nanoparticles in ovarian cancer were limited by failure of *in vitro* studies to translate successfully into *in vivo* efficacy, although two nanoparticle drug delivery systems did perform well in preclinical studies and have reached clinical trials.<sup>11–15</sup> One clinical trial utilized Paclimer microparticles which consist of a sustained-release formulation of paclitaxel-loaded (10 % wt/wt) polyphosphoester particles.<sup>27</sup> In a phase I trial of patients with recurrent ovarian cancer, IP administration was well tolerated and dose-limiting toxicity was not observed, but a significant inflammatory response and adhesions were noted in the only patient to undergo reexploration and no further studies have been reported. The other clinical trial utilized albumin-bound paclitaxel nanoparticles designed to increase intracellular delivery and reduce systemic side effects through trans-endothelial transport via albumin gradients surrounding tumor cells. A phase II trial of these nanoparticles did exhibit reduced toxicity and side effects but improvement in overall survival was minimal.<sup>11</sup> Therefore, a number of other systems designed to increase tumor specificity are in preclinical development. For example, folate-targeted

nanoparticles capable of localizing to ovarian tumors via folate receptors has been shown to deliver both paclitaxel and radiotherapeutics to tumor in a murine model and nanoparticles containing biodegradable polymer complexes delivering suicide DNA to ovarian tumor cells have been described but not yet tested *in vivo*.<sup>12, 14</sup> Whereas these studies are promising, clinical success in ovarian cancer will require these approaches significantly decrease systemic morbidity and/or drastically inhibit local tumor recurrence compared with current paclitaxel therapy after surgical resection.

Our investigation is the first to study the efficacy of drug-eluting pH-responsive nanoparticles in the prevention of local recurrence of ovarian cancer following cytoreductive surgery. The eNP are pH-responsive and designed to swell upon endocytosis, resulting in prolonged drug delivery within the tumor cell with the goal of decreasing systemic side effects. Expansile nanoparticles in our experiment are designed to swell within the endosome at a pH of 5. Ascitic fluid normally has a pH reflective of the pH of blood. Studies of malignant ascites from patients with ovarian cancer have demonstrated pH in the range of 7.3, and rarely below pH 7, which is still significantly higher than the pH found in endosomes at which Pax-eNP have been shown to release drug.<sup>16</sup> This results in paclitaxel release from eNP only occurring after uptake into the endosome and not generally into the ascites where it can be cleared from the body.<sup>33–35</sup> Pax-eNP leads to significant cytotoxicity *in vitro* against the OVCAR-3 human cell line and fresh human ovarian cancer cells retrieved from a multidrug-resistant malignant pleural effusion. Unlike

pax-C/E, which has a plasma half-life of 5 h, pax-eNP are designed to expand upon entry into the endosome and deliver drug inside the tumor cell over a prolonged period of time. Based on the continued intracellular presence of pax-eNP at 24 h seen via flow cytometric analyses and confocal imaging, eNP swelling appears to delay or prevent exocytosis of the eNP thus leading to increased duration, and potentially increased antitumor efficacy. Rapid uptake and continued intracellular presence of eNP at 24 h allows for increased drug delivery to tumor cells and a greater likelihood of drug presence during tumor cell division. Whereas the exact pathway is not known, endocytosis of eNP is an active process as uptake ceases at 4 °C.<sup>28</sup> Studies are currently underway to address the specific endocytotic pathway involved.

Because localization of eNP to tumor would enhance efficacy, we investigated whether eNP would selectively localize to areas of established tumor. In vivo data of rho-eNP demonstrate the ability of eNP to selectively localize to areas of tumor, thereby decreasing systemic toxicity and delivering sustained treatment doses of paclitaxel at locations of established tumor. Compared with intravenous administration, intraperitoneal localization of eNP to tumor sites has the effect of limiting recurrence and avoiding splenomegaly while potentially improving outcomes over surgical resection alone. Although the mechanism for eNP tumor targeting in vivo is unknown, several studies using intravenous nanoparticles have identified leaky capillaries within tumors as a major mechanism of nanoparticles accumulation.<sup>29–32</sup> In this study, however, eNP do not perfuse the tumor via capillaries and thus eNP are localizing to tumor via a surface-based mechanism, most likely the result of a polymeric NP-receptor interaction, a non-specific adhesive attraction, such as charge, or via a metabolic property of in vivo tumor growth. We are currently exploring these possibilities.

Because this was a proof of concept study, all animals were sacrificed when recurrent disease was evident in unloaded eNP controls to allow accurate comparison of the extent of tumor recurrence between groups at the same time point. Intraperitoneal treatment is dependent on absorbance and contact time of the drug with tumor cells. In addition, paclitaxel is only effective in cells actively in mitotic phase and conventional paclitaxel may be exocytosed or transported out of the cell by membrane associated glycoprotein P-gp, which functions as an efflux pump to remove drug from the tumor cell. These properties may result in variable Pax efficacy with resulting responders and nonresponders leading to a high variance between two groups. As a result, mean tumor volumes of responders and nonresponders are equally centered around mean, average tumor volumes, and may not be reliable as a direct comparison. The pax-C/E group demonstrates the expected bimodal distribution of

responders and non-responders with tumor sizes centered around 0.57. Due to the distribution of pax-C/E, we feel there is variable drug delivery and therefore we expect to see responders and nonresponders in a bimodal distribution (hence the rationale for the variance ratio test). Unfortunately, the distributional differences were not large enough to be significant in the setting of this bimodal distribution, but there were several tumors in the pax-c/e group that were substantially larger than any in the Pax-eNP cohort. A two-group variance test to compare if the distributions have different patterns of spread was performed as a way to assess population differences of responders and nonresponders. In these data, the two-sided *p* value for the variance ratio test is 0.0003 with the variance ratio itself equal to 15.7. Therefore, although the mean difference was not significant, there is statistical evidence of a difference in variability of these two populations (pax c/e and pax-eNP). Given that 43 % of pax-C/E animals exhibited significant carcinomatosis at the time of sacrifice (vs. 0 % of pax-eNP animals), survival of pax-eNP treated animals would be expected to be prolonged compared with the other treatment groups, had animals not been sacrificed for comparative analysis. Given the long duration of follow-up required for this particular model, absolute survival benefit will be the focus of a much larger future study.

In the current study, pax-eNP are capable of ovarian tumor cell uptake leading to in vitro cytotoxicity in both a standard cell line and by tumor cells from a malignant pleural effusion. Low morbidity, in vivo localization, and superior inhibition of local tumor recurrence has been demonstrated in a novel cytoreductive murine model of peritoneal carcinomatosis associated with ovarian cancer. The main limitation of this study is the use of a single ovarian cancer line and, as a result, it is difficult to extrapolate to various ovarian cancer cell lines. Recent studies further demonstrate that tumor-localizing eNP can be used as an intratumoral drug depot, whereby intraperitoneal pax-C/E will home to unloaded eNP within the tumor, suggesting that “periodic reloading” of pax-eNP within the tumor may further improve efficacy without the need for repeat application of catheter based therapies.<sup>28</sup> The delivery of paclitaxel directly to sites of ovarian tumor is unique and leads to decreased recurrence and tumor burden, potentially improving outcomes compared with standard local paclitaxel therapy. These results justify additional studies to explore potential clinical feasibility following surgical debulking including long-term survival studies, the assessment of multidose pax-eNP therapy, and depot studies on long-term survival and safety of novel tumor-localized eNP-mediated drug delivery.

**ACKNOWLEDGMENT** The authors express their appreciation to Brigham and Women’s Hospital, the Dana-Farber Cancer Institute



Animal Facility, and Beth Israel Deaconess Medical Center Confocal Imaging Core who kindly provided their expertise and guidance. This work was supported by the Center for Integration of Medicine and Innovative Technology, the Cross-Disciplinary Training in Nanotechnology for Cancer, NIH R25 CA153955, and the NSF DMR-1006601.

**DISCLOSURE** None.

## REFERENCES

- National Cancer Institute. NCI clinical announcement on intraperitoneal chemotherapy in ovarian cancer. 2006. <http://ctep.cancer.gov/highlights/ovarian.html>. Accessed 5 Jan 2006.
- Lewin S, Herzog T, Barrena Medel N, et al. Comparative performance of the new versus old FIGO staging system for endometrial cancer. *Gynecol Oncol*. 2010;116:S6–7.
- Ang C, Chan KKL, Bryant A, et al. Ultra-radical (extensive) surgery versus standard surgery for the primary cytoreduction of advanced epithelial ovarian cancer. *Cochrane Database Syst Rev*. 2011;(4):CD007697. doi:10.1002/14651858.CD007697.pub2.
- Howlander N, Noone AM, Krapcho M, et al. SEER cancer statistics review, 1975–2008. Bethesda: National Cancer Institute; 2011.
- Jemal A, Siegel R, Ward E, et al. Cancer statistics, 2007. *CA Cancer J Clin*. 2007;57(1):43–66.
- du Bois A, Quinn M, Thigpen T, et al. 2004 Consensus statements on the management of ovarian cancer: final document of the 3rd International Gynecologic Cancer Intergroup Ovarian Cancer Consensus Conference (GCI/OCCC 2004). *Ann Oncol*. 2005;16 (Suppl 8):viii7–12.
- Armstrong DK, Bundy B, Wenzel L, et al. Intraperitoneal cisplatin and paclitaxel in ovarian cancer. *N Engl J Med*. 2006;354(1):34–43.
- Walker J, Armstrong DK, Huang HK, et al. Intraperitoneal catheter outcomes in a phase III trial of intravenous versus intraperitoneal chemotherapy in optimal stage III ovarian and primary peritoneal cancer: a Gynecologic Oncology Group study. *Gynecol Oncol*. 2006;100(1):27–32.
- Ozols RF, Bundy BN, Greer BE, et al. Phase III trial of carboplatin and paclitaxel compared with cisplatin and paclitaxel in patients with optimally resected stage III ovarian cancer: a Gynecologic Oncology Group study. *J Clin Oncol*. 2003;21(17):3194–200.
- Kirmani S, Braly PS, McClay EF, et al. A comparison of intravenous versus intraperitoneal chemotherapy for the initial treatment of ovarian cancer. *Gynecol Oncol*. 1994;54 (3):338–44.
- Coleman, Brady, McMeekin, et al. A phase II evaluation of nanoparticle, albumin-bound (nab) paclitaxel in the treatment of recurrent or persistent platinum-resistant ovarian, fallopian tube, or primary peritoneal cancer: a Gynecologic Oncology Group study. *Gynecol Oncol*. 2011;122 (1):111–5.
- Werner ME, Karve S, Sukumar R, et al. Folate-targeted nanoparticle delivery of chemo- and radiotherapeutics for the treatment of ovarian cancer peritoneal metastasis. *Biomaterials*. 2011;32 (33):8548–54.
- Sloat BR, Sandoval MA, Li D, et al. In vitro and in vivo anti-tumor activities of a gemcitabine derivative carried by nanoparticles. *Int J Pharm*. 2011;409 (1–2):278–88.
- Sawicki JA, Anderson DG, Langer R. Nanoparticle delivery of suicide DNA for epithelial ovarian cancer therapy. *Adv Exp Med Biol*. 2008;622:209–19.
- Schulz MD, Zubris KA, Wade JE, et al. Paclitaxel-loaded expansile nanoparticles in a multimodal treatment model of malignant mesothelioma. *Ann Thorac Surg*. 2011;92 (6):2007–13.
- Griset AP, Walpole J, Liu R, et al. Expansile nanoparticles: synthesis, characterization, and in vivo efficacy of an acid responsive polymeric drug delivery system. *J Am Chem Soc*. 2009;131:2469–71.
- Hamilton TC, Young RC, Louie KG, et al. Characterization of a xenograft model of human ovarian carcinoma which produces ascites and intraabdominal carcinomatosis in mice. *Cancer Res*. 1984;44:5286–90.
- Massazza G, Tomasoni A, Lucchini V, et al. Intraperitoneal and subcutaneous xenografts of human ovarian carcinoma in nude mice and their potential in experimental therapy. *Int J Cancer*. 1989;44:494–500.
- Joerger M, et al. Population pharmacokinetics and pharmacodynamics of paclitaxel and carboplatin in ovarian cancer patients: a study by the European Organization for Research and Treatment of Cancer-Pharmacology and Molecular Mechanisms Group and New Drug Development Group. *Clin Cancer Res*. 2007;13:6410.
- Yen MS, Juang CM, Lai CR, et al. Intraperitoneal cisplatin-based chemotherapy vs. intravenous cisplatin-based chemotherapy for stage III optimally cytoreduced epithelial ovarian cancer. *Int J Gynaecol Obstet*. 2001;72 (1):55–60.
- Konner JA, Grabon D, Pezzulli S, et al. A phase II study of intravenous (IV) and intraperitoneal (IP) paclitaxel, IP cisplatin, and IV bevacizumab as first-line chemotherapy for optimal stage II or III ovarian, primary peritoneal, and fallopian tube cancer [abstract]. *J Clin Oncol*. 2009;27:5539.
- Hoskins WJ, McGuire WP, Brady MF, et al. The effect of diameter of largest residual disease on survival after primary cytoreductive surgery in patients with suboptimal residual epithelial ovarian carcinoma. *Am J Obstet Gynecol*. 1994;170 (4):974–9.
- Hoskins WJ, Bundy BN, Thigpen JT, et al. The influence of cytoreductive surgery on recurrence-free interval and survival in small-volume stage III epithelial ovarian cancer: a Gynecologic Oncology Group study. *Gynecol Oncol*. 1992;47 (2):159–66.
- Bristow RE, Tomacruz RS, Armstrong DK, et al. Survival effect of maximal cytoreductive surgery for advanced ovarian carcinoma during the platinum era: a meta-analysis. *J Clin Oncol*. 2002;20 (5):1248–59.
- Araujo L, Lobenberg R, Kreuter J. Influence of the surfactant concentration on the body distribution of nanoparticles. *J Drug Targeting*. 1999;6:373–85.
- Armstrong DK, Fleming GF, Markman M, Bailey HH. A phase I trial of intraperitoneal sustained-release paclitaxel microspheres (Paclimer) in recurrent ovarian cancer: a Gynecologic Oncology Group study. *Gynecol Oncol*. 2006;103:391–6.
- Zubris KA, Colson YL, Grinstaff MW. Hydrogels as intracellular depots for drug delivery. *Mol Pharm*. 2012;9(1):196–200.
- Lammers T, Hannink WE, Storm G. Tumour-targeted nanomedicines: principles and practice. *Br J Cancer*. 2008;99(3):392–7.
- Peer D, Karp JM, Hong S, et al. Nanocarriers as an emerging platform for cancer therapy. *Nat Nanotechnol*. 2007;2:751–60.
- Kim BY, Rutka JT, Chan WC, et al. Nanomedicine. *N Engl J Med*. 2010;363:2434–43.
- Gilmore D, Colson YL. Tumor targeted nanoparticles: a modern day Trojan horse. *Semin Thorac Cardiovasc Surg*. 2011;23(1):10–11.
- Yang CY, Liaw YF, Chu CM, Sheen IS. White count, pH and lactate in ascites in the diagnosis of spontaneous bacterial peritonitis. *Hepatology*. 1985;5(1):85–90.
- Emoto S, Kitayama J, Yamaguchi H, Ishigami H, Kaisaki S, Nagawa H. Analysis of pO<sub>2</sub> in malignant ascites of patients with

- peritoneal dissemination of gastric cancer. *Case Rep Oncol.* 2010;3:344–8.
34. Wike-Hooley JL, Haveman J, Reinhold HS. The relevance of tumour pH to the treatment of malignant disease. *Radiother Oncol.* 1984;2:343–66.
35. Boyer MJ, Tannock IF. Regulation of intracellular pH in tumor cell lines: influence of microenvironmental conditions. *Cancer Res.* 1992;52:4441–7.